SARS-CoV-2 Infection and Transmission Depends on Heparan Sulfates and Is Blocked by Low Molecular Weight Heparins

Marta Bermejo-Jambrina[1†], Julia Eder[1†], Tanja M. Kaptein[1], Leanne C. Helgers[1], Philip J.M. Brouwer[2], John L. van Hamme[1], Alexander P.J. Vlaar[3], Frank E.H.P. van Baarle[3], Godelieve J. de Bree[4], Bernadien M. Nijmeijer[1], Neeltje A. Koostra[1], Marit J. van Gils[2], Rogier W. Sanders[2,5], Teunis B. H. Geijtenbeek[1*]

[1]Department of Experimental Immunology, Amsterdam institute for Infection and Immunity, Amsterdam University Medical Centers, University of Amsterdam, Meibergdreef 9, Amsterdam, The Netherlands.

[2]Department of Medical Microbiology, Amsterdam institute for Infection and Immunity, Amsterdam University Medical Centers, University of Amsterdam, Meibergdreef 9, Amsterdam, The Netherlands.

[3]Department of Intensive Care Medicine, Amsterdam University Medical Centers, University of Amsterdam, Meibergdreef 9, Amsterdam, The Netherlands.

[4]Department of Internal Medicine, Amsterdam institute for Infection and Immunity, Amsterdam University Medical Centers, University of Amsterdam, Meibergdreef 9, Amsterdam, The Netherlands.

[5]Department of Microbiology and Immunology, Weill Medical College of Cornell University, New York, NY 10021, USA.

* Corresponding author:
Prof. dr. Teunis B.H. Geijtenbeek, phone: +31 (0)20 56 66063, email: t.b.geijtenbeek@amsterdamumc.nl, Department of Experimental Immunology, Amsterdam University Medical Centers, location AMC, University of Amsterdam, Meibergdreef 9, 1105 AZ, Amsterdam, The Netherlands

† These authors contributed equally.

Keywords: SARS-CoV-2, Syndecans, attachment block, inhibit infection, epithelial cells

Abstract

The current pandemic caused by severe acute respiratory syndrome coronavirus-2 (SARS-CoV-2) and new outbreaks worldwide highlight the need for preventive treatments. Although angiotensin converting enzyme 2 (ACE2) is the primary receptor for SARS-CoV-2, we identified heparan sulfate proteoglycans expressed by epithelial cells, alveolar macrophages and dendritic cells as co-receptors for SARS-CoV-2. Low molecular weight heparins (LMWH) blocked SARS-CoV-2 infection of epithelial cells and alveolar macrophages, and virus dissemination by dendritic cells. Notably, potent neutralizing antibodies from COVID-19 patients interfered with SARS-CoV-2 binding to heparan sulfate proteoglycans, underscoring the importance of heparan sulfate proteoglycans as receptors and uncover that SARS-CoV-2 binding to heparan sulfates is an important mechanism for neutralization. These results have imperative implications for our understanding of SARS-CoV-2 host cell entry and reveal an important target for novel prophylactic intervention.

Introduction

Severe acute respiratory syndrome coronavirus 2 (SARS-CoV-2) emerged in Wuhan, China in late 2019 and can cause coronavirus disease 2019 (COVID-19), an influenza-like disease ranging from mild respiratory symptoms to severe lung injury, multi organ failure and death (1-3). SARS-CoV-2 spread quickly and has caused a pandemic with a severe impact on global health and world economy (4, 5). SARS-CoV-2 is transmitted predominantly via large droplets expelled from the upper respiratory tract through sneezing and coughing (6, 7) and is subsequently taken up via mucosal surfaces of the nose, mouth and eyes (8). SARS-CoV-2 infects epithelial cells in the respiratory tract, such as ciliated mucus secreting bronchial epithelial cells and type 1 pneumocytes in the lung, as well as epithelial cells in the gastrointestinal tract (9, 10). To date, there is no treatment to prevent SARS-CoV-2 infection. Lockdown strategies and social distancing mitigate viral spread but due to negative socioeconomic consequences these are not feasible long-term solutions (11, 12). Recent renewed outbreaks underscore the urgent need for protective strategies specifically targeting SARS-CoV-2 to prevent further dissemination.

SARS-CoV-2 belongs to the betacoronaviruses, a family that also includes SARS-CoV and MERS-CoV (13). The coronavirus Spike (S) protein is a class I fusion protein that mediates virus entry (14, 15). The S protein consist of two subunits; S1 directly engages via its receptor-binding domain (RBD) with host surface receptors (16, 17) and S2 mediates fusion between virus and cell membrane (18, 19). SARS-CoV-2 uses angiotensin-converting enzyme 2 (ACE2) as its main receptor (13, 20). ACE2 is a type I integral membrane protein abundantly expressed on epithelial cells lining the respiratory tract (21) but also the ileum, esophagus and liver (22) and ACE2 expression dictates SARS-CoV-2 tropism (10). However, it remains unclear whether SARS-CoV2 requires other receptors for virus entry. Neutralizing monoclonal antibodies against SARS-CoV-2 have been identified that are directed not only at the RBD but also outside the RBD (23), supporting the presence of other receptors. Here we show that the heparan sulfate proteoglycans (HSPG) Syndecan 1 and 4 are required for SARS-CoV-2 infection of permissive cells, and that low molecular weight heparins (LMWH) efficiently inhibited infection of polarized epithelial cells as well as alveolar macrophages. Moreover, we show that primary DC subsets use HSPG as attachment receptors to facilitate dissemination of

80 SARS-CoV-2. These findings are important to develop prophylactics against SARS-CoV-
81 2 or prevent dissemination early after infection.
82
83 **Results**

84 **Heparan sulfate proteoglycans are crucial for SARS-CoV-2 binding and infection**
85 Heparan sulfates are expressed by most cells including epithelial cells as heparan sulfate
86 proteoglycans and these have been shown to interact with viruses such as HIV-1, HCV,
87 Sindbis virus and also SARS-CoV (24-28). We incubated Huh 7.5 cells that express ACE2
88 (Supplementary Fig. 1A) with SARS-CoV-2 pseudovirus (23) and observed strong binding
89 of SARS-CoV-2 pseudovirus to cells (Fig. 1A). Binding of SARS-CoV-2 was inhibited by
90 a blocking antibody against ACE2 (Fig. 1A). Moreover, SARS-CoV-2 pseudovirus binding
91 was inhibited by neutralizing antibodies from COVID-19 patients directed against the RBD
92 (COVA1-18, COVA2-15) and non-RBD (COVA1-21) epitopes of the SARS-CoV-2 S
93 protein (23). Notably, unfractionated (UF) heparin potently inhibited the binding of SARS-
94 CoV-2 pseudovirus to cells comparable to the antibody against ACE2 (Fig. 1B).
95 Enzymatic removal of heparan sulfates on the cell surface by Heparinase treatment
96 decreased SARS-CoV-2 virus binding (Fig. 1C and Supplementary Fig. 1B). Furthermore,
97 we observed that SARS-CoV-2 pseudovirus infected Huh 7.5 cells, which was blocked by
98 UF heparin (Fig. 1D). These data strongly suggest that SARS-CoV-2 requires heparan
99 sulfates to infect ACE2-positive cells.
100
101 **Low molecular weight heparins inhibit SARS-CoV-2 infection**
102 Low molecular weight heparin (LMWH) have replaced UF heparin in the clinic as anti-
103 coagulant treatment due to their smaller size and superior pharmacological properties (29)
104 Importantly, LMWH therapy has recently been shown to decrease mortality in severely ill
105 COVID-19 patients (30) and is now used as anti-coagulant prophylaxis for COVID-19
106 patients. Several LMWH are used clinically and differ in size and preparation (31). We
107 therefore screened different LMWHs for their ability to block SARS-CoV-2 binding and
108 infection. All LMWH tested blocked SARS-CoV-2 binding to Huh 7.5 cells and inhibition
109 was similar to that of UF heparin (Fig. 2A). Moreover, the different LMWH inhibited
110 infection of Huh 7.5 cells with SARS-CoV-2 pseudovirus in a dose dependent manner

111 (Fig. 2B). Thus, we have identified LMWH as inhibitors of SARS-CoV-2 binding and
112 infection.
113
114 **SARS-CoV-2 infection of epithelial cells is blocked by UF heparin and LMWH**
115 Human kidney epithelial 293T cells with ectopic expression of ACE2 have been used by
116 different studies to investigate the role of ACE2 in SARS-CoV-2 infection ((20, 32) and
117 Supplementary Fig. 1C). Ectopic expression of ACE2 on 293T cells rendered these cells
118 susceptible to SARS-CoV-2 pseudovirus infection but infection was abrogated by both
119 LMWH enoxaparin and UF heparin to a similar level as antibodies against ACE2 (Fig. 3A).
120 The combination of ACE2 antibodies and LMWH enoxaparin or UF heparin fully blocked
121 infection of 293T-ACE2 cells (Fig. 3A). These data strongly suggest that heparan sulfates
122 play a crucial role in SARS-CoV-2 infection.
123 Epithelial cells expressing ACE2 are thought to be primary target cells for SARS-CoV-2
124 infection in the lung and intestinal tract (21, 33). Non-polarized human colon carcinoma
125 Caco-2 cells efficiently bound SARS-CoV-2 pseudovirus (Fig. 3B). Treatment with
126 antibodies against ACE2, UF heparin and LMWH enoxaparin blocked virus binding to the
127 epithelial cell line. Non-polarized epithelial cells express low levels of ACE2 ((34) and
128 Supplementary Fig. 1C) and Caco2 cells were infected by SARS-CoV-2 pseudovirus albeit
129 at a low level. LMWH enoxaparin blocked infection of Caco2 cells similar as antibodies
130 against ACE2 (Fig. 3C). Combining ACE2 antibodies with UF heparin or LMWH
131 enoxaparin did not further increase block in non-polarized Caco2 (Fig. 3B and C). Next
132 we cultured Caco-2 cells on a microporous filter and infected the cells with SARS-CoV-2
133 pseudovirus once they had formed a highly polarized epithelial monolayer. The polarized
134 Caco-2 cells were permissive to infection, which was significantly blocked by LMWH
135 treatment to a similar level as antibodies against ACE2 (Fig. 3D). The combination of an
136 antibody against ACE2 together with LMWH enoxaparin showed the same pattern as each
137 treatment independently (Fig. 3D). These data suggest that heparan sulfates are required
138 for SARS-CoV-2 infection of (non-)polarized epithelial cells.
139
140 **Heparan sulfates are required for transmission by primary dendritic cells**
141 SARS-CoV-2 infects cells in nasal mucosa, lung and the intestinal tract but mechanisms
142 for dissemination of the virus from the respiratory and intestinal tract are still unclear. It
143 has been suggested that macrophages become infected by SARS-CoV-2 (35), which

144 might promote dissemination. Notably, alveolar macrophages isolated by bronchoalveolar
145 lavage were infected by SARS-CoV-2 (Fig 4A). Importantly, LMWH enoxaparin inhibited
146 infection of primary alveolar macrophages with SARS-CoV-2 (Fig. 4A).Different dendritic
147 cell (DC) subsets have been shown to be involved in dissemination of various viruses
148 including SARS-CoV (36-38). We differentiated monocytes to DC, which is a model for
149 submucosal DC, and also isolated primary human Langerhans cells (LCs) from skin (39,
150 40) as this DC subset resides in epidermis of skin and squamous mucosa of different
151 tissues (41). Both DC and LC efficiently bound SARS-CoV-2 pseudovirus and binding was
152 inhibited by UF heparin as well as LMWH enoxaparin (Fig. 4B and C). Neither DC nor LC
153 expressed ACE2 (Supplementary Fig. 1A) and, SARS-CoV-2 pseudovirus did not infect
154 DC nor LC (Fig. 4D and E). However, DC subsets are able to transmit HIV-1 to target cells
155 independent of productive infection (40, 42). We therefore treated DC and LC with SARS-
156 CoV-2 pseudovirus and after washing co-cultured the cells with susceptible Huh 7.5 cells.
157 Notably, both DCs and LCs efficiently transmitted captured SARS-CoV-2 to Huh 7.5 cells
158 and transmission was blocked by UF heparin as well as LMWH enoxaparin pre-treatment
159 (Fig. 4F and G). Thus, our data strongly suggest that DC subsets are involved in virus
160 dissemination of SARS- CoV-2 independent of direct infection and in a heparan sulfate-
161 dependent manner.
162
163 **Heparan sulfate proteoglycans Syndecan 1 and 4 are important for SARS-CoV-2**
164 **binding and infection**
165 The heparan sulfate proteoglycan family of Syndecans are particularly important in
166 facilitating cell adhesion of several viruses (28, 43). Therefore we investigated SARS-CoV-
167 2 binding to Namalwa cells expressing Syndecan 1 and 4 (Supplementary Fig. 2A) as
168 these Syndecans are expressed by epithelial cells (44, 45). Namalwa cells did not express
169 ACE2 (Supplementary Fig. 1A). SARS-CoV-2 pseudovirus bound to Syndecan 1 and 4
170 transduced cell-lines with higher efficiency than the parental cell-line (Fig. 5A and
171 (Supplementary Fig. 2A). UF heparin and LMWH enoxaparin blocked the interaction of
172 Syndecan 1 and 4 with SARS-CoV-2 pseudovirus (Fig. 5A).
173 Epithelial cells (44, 45) and Huh 7.5 cells express Syndecan 1 and 4 and we silenced both
174 Syndecan 1 and 4 by RNA interference (Supplementary Fig. 2B). Notably, silencing of
175 Syndecan 1 or Syndecan 4 decreased SARS-CoV-2 infection of Huh 7.5 cells (Fig. 5B)
176 supporting a role for Syndecan 1 and 4 in SARS-CoV-2 infection. These data indicate that

177 Syndecan 1 and 4 are the main heparan sulfate proteoglycans involved in SARS-CoV-2
178 binding and infection.
179
180 **Potent neutralizing antibodies against SARS-CoV-2 S protein target heparan**
181 **sulfate-SARS-CoV-2 interactions**
182 Recently several potent neutralizing antibodies against SARS-CoV-2 have been isolated
183 from COVID-19 patients that target the RBD (COVA1-15, COVA1-18) as well as the non-
184 RBD (COVA1- 21) of the S protein (23). In order to investigate whether these antibodies
185 can prevent binding of SARS-CoV-2 to heparan sulfates, we examined their ability to
186 inhibit virus binding to ACE2-negative Namalwa cells expressing Syndecan 1. Notably,
187 the two RBD and the non-RBD binding antibodies blocked the interaction of SARS-CoV-
188 2 pseudovirus with Syndecan 1 to a similar extent as LMWH (Fig. 6A). In contrast, the
189 isotype antibodies did not inhibit virus binding.
190 To investigate whether these antibodies specifically block the interaction of SARS-CoV-2
191 with heparan sulfates, we coated UF heparin and measured SARS-CoV-2 S protein
192 binding. SARS- CoV-2 S protein efficiently bound to coated heparin (Fig. 6B). All three
193 antibodies against S protein blocked the interaction of heparin with SARS-CoV-2, strongly
194 suggesting that the neutralizing antibodies against SARS-CoV-2 interfere with heparan
195 sulfate binding by the virus. Thus, our data strongly suggest that neutralization by
196 antibodies against SARS-CoV-2 can occur via ACE2 inhibition but also by preventing
197 SARS-CoV-2 binding to heparan sulfate proteoglycans, and underscores the importance
198 of heparan sulfate proteoglycans in infection.
199
200 **Discussion**

201 Here we have shown that SARS-CoV-2 infection is not only dependent on ACE2 but also
202 requires heparan sulfate proteoglycans and in particular Syndecan 1 and 4. Our data
203 suggest that SARS-CoV-2 attaches to cells via HSPG, which facilitates thereby interaction
204 with ACE2 and subsequent infection. Moreover, we also identified HSPG as important
205 receptors facilitating ACE2-independent transmission by primary DCs. Infection as well as
206 transmission with SARS-CoV-2 was efficiently inhibited by the clinically adapted UF
207 heparin and LMWH. It further suggests that neutralizing antibodies isolated from COVID-
208 19 patients could at least partially inhibit SARS- CoV- 2 binding to heparan sulfate

209 proteoglycans and thereby interfere with infection. These results have important
210 implications for our understanding of SARS-CoV-2 host cell entry and reveal a relevant
211 target for novel prophylactic intervention.
212
213 Recently, is has been suggested that the SARS-CoV-2 S protein interacts with heparan
214 sulfate molecules and heparin (46-48). Here we have identified heparan sulfates and in
215 particular Syndecan 1 and 4 as important receptors for SARS-CoV-2. Our data strongly
216 suggest that the heparan sulfate proteoglycans are required for virus binding and infection
217 of epithelial cells. LMWH or UF heparin efficiently abrogated virus infection to a similar
218 extent as ACE2 antibodies and combinations of ACE2 antibodies, suggesting that both
219 receptors are required for virus infection. To investigate the role of SARS-CoV-2 infection
220 in primary cells, we isolated alveolar macrophages and epidermal LCs, and cultured
221 monocyte-derived DCs. Interestingly, alveolar macrophages were infected by SARS-CoV-
222 2 in a HSPG dependent manner whereas neither LCs nor DCs were infected. The role of
223 alveolar macrophages in SARS-CoV-2 infection is still unclear but it has been
224 hypothesized that they can infiltrate other tissues or induce pro-inflammatory cytokines
225 and chemokines upon infection (49), indicating a potential detrimental role in disease
226 progression. Interestingly, infection of primary alveolar macrophages isolated from lung
227 was also inhibited by LMWH, suggesting an important role for LMWH protection in lung
228 tissue not as an anti-coagulant but as an antiviral.
229 DCs migrate from mucosal tissues and epidermis into lymphoid tissues (50) and therefore
230 it is thought that DCs are involved in the dissemination of viruses after infection (51). Our
231 data strongly suggest that DCs similarly are involved in SARS-CoV-2 dissemination via
232 HSPG as primary DC subsets isolated from skin or derived from blood monocytes strongly
233 bound SARS-CoV-2 via HSPG and efficiently transmitted the virus to target epithelial cells.
234 The HSPG cell surface receptor primarily expressed by epithelial cells is Syndecan 1 (44,
235 52) and is involved in cell recruitment, proliferation and inflammations (45) but can also
236 bind viruses like Herpes simplex virus (HSV-1) (43) and Hepatitis C virus (53). Syndecan
237 4 is further expressed ubiquitously albeit at lower levels (45). Recently we could show that
238 Syndecan 4 is involved in transmission of HCV by LCs (28) whereas Syndecan 3 facilitates
239 binding and transmission of HIV-1 (54). In this study we demonstrate the interaction of
240 specific Syndecans with SARS-CoV-2 and underscore their importance for virus
241 attachment and dissemination.

242 Neutralizing antibodies against SARS-CoV-2 are a potential therapy for COVID-19
243 patients and several potent monoclonal neutralizing antibodies have been identified that
244 target the RBD and non-RBD sites of the S protein of SARS-CoV-2 (23). However, while
245 most of the antibodies are suggested to inhibit ACE2 binding sites, the non-RBD
246 antibodies COVA1-21 does not seem to interfere with ACE2 and instead interfere with
247 other COVA antibodies and as yet unidentified receptors. Notably, two RBD antibodies
248 COVA1-18 and COVA2-15 blocked virus as well as S protein binding to heparan sulfates,
249 indicating that the RBD is also involved in heparan sulfate interactions (23). Moreover, our
250 data suggest that COVA1-21 targets the heparan binding site of the S protein. Recent
251 studies suggest that the heparan sulfate binding site of the S protein are outside the RBD
252 of SARS-CoV-2 (47, 48). The finding that neutralizing antibodies against SARS-CoV-2
253 block heparan sulfate interactions suggest that this is an important target for neutralization
254 of the and underscores the importance of the interaction for SARS-CoV-2 infection. Thus
255 this finding shows that the unusually potent antibodies COVA1-18 and 2-15 can neutralize
256 SARS-CoV-2 through two mechanisms: preventing SARS-CoV-2 binding to ACE2 (23)
257 and to heparan sulfate proteoglycans.
258 LMWHs are already used as subcutaneous treatment of COVID-19 patients to prevent
259 systemic clotting (55, 56). Interestingly, here we have identified an important ability of
260 LMWH to directly block SARS-CoV-2 binding and infection of epithelial cells as well as
261 preventing virus transmission. Our data support the use of LMWH as prophylactic
262 treatment for SARS-CoV-2 as well as a treatment option early in infection to block further
263 infection and dissemination. LMWH inhalation has been studied to attenuate inflammatory
264 responses in COPD and asthma patients and is considered safe to use as a prophylactic.
265 The clinical use of LMWH to treat COVID-19 and our finding that LMWH block virus
266 infection and dissemination strongly advocate for the prophylactic use of LMWH in
267 individuals at risk for infection, or short after infection or even for a general population
268 during outbreaks we still observe daily to quickly limit transmission events.
269 In summary, this study provided new insights into how SARS-CoV-2 initiates attachment,
270 infection and transmission in different cell types and showed that LMWH are possible
271 candidates for prophylactic intervention and antiviral treatment.
272
273
274

275 **Materials and Methods**

276 *Virus production*

277 For production of single-round infection viruses, human embryonic kidney 293T/17 cells
278 (ATCC, CRL-11268) were co-transfected with an adjusted HIV backbone plasmid (pNL4-
279 3.Luc.R-S-) containing previously described stabilizing mutations in the capsid protein
280 (PMID: 12547912) and firefly luciferase in the *nef* open reading frame (1.35ug) and
281 pSARS-CoV-2 expressing SARS-CoV-2 S protein (0.6ug) (GenBank; MN908947.3) (23).
282 Transfection was performed in 293T/17 cells using genejuice (Novagen, USA) transfection
283 kit according to manufacturer's protocol. At day 3 or day 4, pseudotyped SARS-CoV-2
284 virus particles were harvested and filtered over a 0.45 µm nitrocellulose membrane
285 (SartoriusStedim, Gottingen, Germany).
286 SARS-CoV-2 pseudovirus productions were quantified by p24 ELISA (Perkin Elmer Life
287 Sciences).
288

289 *Reagents and antibodies*

290 The following antibodies were used (all anti-human): ACE-2 (R&D), (Heparan Sulfate
291 (clone F58-10E4) (Amsbio), digested Heparan (clone F69-3G10) (Amsbio), CD1a-APC
292 mouse IgG1 (BD Biosciences, San Jose, CA, USA), CD207-PE (langerin) mouse IgG1
293 (#IM3577) FITC-conjugated goat-anti-mouse IgM (#31992) (Invitrogen), AF488-
294 conjugated donkey-anti-mouse IgG2b (Invitrogen), Flow cytometric analyses were
295 performed on a BD FACS Canto II (BD Biosciences). Data was analyzed using FlowJo
296 vX.0.7 software (TreeStar).
297 The following reagents were used: Unfractionated (UF) heparin, 5.000 I.E./ml (LEO). Low
298 Molecular Weight heparins (LMWH): dalteparin, 10.000 IE anti-Xa/ml (Pfizer), tinzaparin,
299 10.000 IE anti-X1/0.5ml (LEO), enoxaparin, 6000 IE (60mg)/0.6 ml (Sanofi), nadroparin,
300 9.500 IE anti-XA/ml (Aspen). Heparinase III from *Flavobacterium heparium*, EC 4.2.2.8,
301 Batch 010, (Amsbio). Biotinylated SARS-CoV-2 S protein as well as neutralizing
302 antibodies COVA1-18, COVA-1-21 and COVA-2-15 were generated as described
303 previously (23).
304
305
306

307 *Cell lines*

308 The human B cell line Namalwa (ATCC, CRL-1432) and Namalwa cells stably expressing
309 human Syndecan 1 and Syndecan 4 (57) were a gift from Dr. Guido David and Dr. Philippe
310 A Gallay. The cells were maintained in RPMI 1640 medium (Gibco Life Technologies,
311 Gaithersburg, Md.) containing 10% fetal calf serum (FCS), penicillin/streptomycin
312 (10 µg/ml) and 1 mM sodium pyruvate (Thermo Fisher). The expression of the different
313 Syndecans was validated by PCR analysis using specific primers aimed against
314 Syndecans. Huh7.5 (human hepatocellular carcinoma) cells received from dr. Charles M.
315 Rice (58) were maintained in Dulbecco modified Eagle medium (Gibco Life Technologies,
316 Gaithersburg, Md.) containing 10% fetal calf serum (FCS), L-glutamine and
317 penicillin/streptomycin (10 µg/ml). Medium was supplemented with 1mM Hepes buffer
318 (Gibco Life Technologies, Gaithersburg, Md.). The human embryonic kidney 293T/17 cells
319 (ATCC, CRL-11268) were maintained in maintained in Dulbecco modified Eagle medium
320 (Gibco Life Technologies, Gaithersburg, Md.) containing 10% fetal calf serum (FCS), L-
321 glutamine and penicillin/streptomycin (10 µg/ml). The human epithelial Caco2 cells
322 (ATCC, HTB-37™) were maintained in Dulbecco modified Eagle medium (Gibco Life
323 Technologies, Gaithersburg, Md.) containing 10% fetal calf serum (FCS), L-glutamine and
324 penicillin/streptomycin (10 µg/ml) and supplemented with MEM Non-Essential Amino
325 Acids Solution (NEAA) (Gibco Life Technologies, Gaithersburg, Md.). To create a
326 monolayer of polarized cells, Caco2 cells were maintained in 6.5 mm transwells with a 5
327 µm Pore Polycarbonate Membrane Insert (Corning). The cells were initially seeded with a
328 density of 25.000 cells per 6.5 mm filter insert and full polarization was reached after 4
329 weeks in culture.

330

331 *SARS-CoV-2 S protein binding ELISA*

332 UF Heparin (diluted in PBS) was coated using high binding ELISA plates for 2h at 37°C.
333 Non-specific binding was blocked by incubating the plate 1% BSA in TSM (20 mM Tris–
334 HCl, pH 7.4, containing 150 mM NaCl, 2 mM CaCl2, and 2 mM MgCl2) for 30 min at 37
335 °C. Biotinylated Spike protein was pre-incubated with different antibodies (20 µg/ml) for
336 30 min at RT. Biotinylated SARS-CoV-2 S protein was added for 2 hours at RT. Unbound
337 Spike protein was washed away and streptavidin-HRP (1/10000) (Thermofisher) was
338 added. After washing, a TMB/hydrogen peroxide substrate was added for color
339 development. This reaction was stopped by adding 0.8 M H2SO4 and the optical density

340 was measured at 450 nm. Negative control included isotype-matched HIV-1 antibody
341 VRC01 (59).
342
343 *293T Transfection with ACE2*
344 To generate cells expressing human ACE2, human embryonic kidney 293T/17 cells were
345 transfected with pcDNA3.1(-)hACE2 (Addgene plasmid #1786). Transfection was
346 performed in 293T/17 cells using the genejuice (Novagen, USA) transfection kit according
347 to manufacturer's protocol. At 24h post-transfection, cells were washed with phosphate-
348 buffered saline (PBS) and cultured for recovering at 37C for 24h in Dulbecco's MEM
349 supplemented with 10% heat-inactivated fetal calf serum (FCS), L-glutamine and
350 penicillin/streptomycin (10 U/ml) After 24h of recovery, cells were cultured in media
351 supplemented with G418 (5mg/mL) (Thermo Fisher) and passage for 3 weeks at 37C.
352 Surviving clones were analyzed for ACE2 expression via flow cytometry and PCR.
353
354 *Virus binding and sensitive p24 ELISA*
355 In order to determine SARS-CoV-2 binding, target cells were exposed to 95 ng of
356 pseudotyped SARS-CoV-2 virus for 4 hours at 4°C. Cells were washed to remove the
357 unbound virus and lysed with lysis buffer. Binding and internalization was quantified by
358 RETRO-TEK HIV-1 p24 ELISA according to manufacturer instructions (ZeptoMetrix
359 Corporation).
360
361 *Infection assays*
362 HuH7.5, 293T(+hACE2) and undifferentiated Caco2 were exposed to 95 ng of
363 pseudotyped SARS-CoV-2 and polarized Caco2 cells to 477.62 ng of pseudotyped SARS-
364 CoV-2. Virus was pre-incubated with 250U LMWH or UF heparin prior to addition of cells.
365 Infection was measured after 5 days at 37°C by the Luciferase assay system (Promega,
366 USA) according to manufacturer's instructions.
367
368 *Primary human cells*
369 CD14+ monocytes were isolated from the blood of healthy volunteer donors (Sanquin
370 blood bank) and subsequently differentiated into monocyte-derived DCs as described
371 previously (60). Epidermal sheets were prepared as described previously (39, 40). Briefly,
372 skin-grafts were obtained using a dermatome (Zimmer Biomet, Indiana USA). After

373 incubation with Dispase II (1 U/ml, Roche Diagnostics), epidermal sheets were separated
374 from dermis, washed and cultured in IMDM (Thermo Fischer Scientific, USA)
375 supplemented with 10% FCS, gentamycine (20 µg/ml, Centrafarm, Netherlands),
376 pencilline/streptomycin (10 U/ml and 10 µg/ml, respectively; Invitrogen) for 3 days after
377 which LCs were harvested. Purity of LCs was routinely verified by flow cytometry using
378 antibodies directed against CD207 (langerin) and CD1a.
379 Alveolar macrophages were prepared from broncheo-alveolar lavage (BAL) fluid that was
380 obtained as spare material from the ongoing DIVA study (Netherlands Trial Register:
381 NL6318; AMC Medical Ethical Committee approval number: 2014_294). The DIVA study
382 includes healthy male volunteers aged 18-35. In this study, the subjects are given a first
383 hit of lipopolysaccharide (LPS) and, two hours later, a second hit of either fresh or aged
384 platelet concentrate or NaCl 0.9%. Six hours after the second hit, a BAL is performed by
385 a trained pulmonologist according to national guidelines. Fractions 2-8 are pooled and
386 split in two, one half is centrifuged (4 °C, 1750 G, 10 min.), the cell pellet of which was
387 used in this research. Since the COVID-19 pandemic, subjects are also screened for
388 SARS-CoV-2 (via throat swab PCR) 2 days prior to the BAL. All subjects in the DIVA study
389 have signed an informed consent form. Cells were washed and plated. After two hours the
390 wells were washed to remove non-adherent cells and adherent macrophages were
391 infected.
392
393 *Transmission assays and co-culture*
394 Alveolar macrophages, DCs or LCs were exposed to 191.05 ng of pseudotyped SARS-
395 CoV-2 or pseudotyped SARS-CoV-2 pre-incubated with 250U UF heparin or LMWH for 4
396 hours, harvested, extensively washed to remove unbound virus and co-cultured with
397 Huh7.5 for 5 days at 37°C after which they were analyzed for with the Luciferase assay
398 system (Promega, USA) according to manufacturer's instructions.
399
400 *RNA isolation and quantitative real-time PCR*
401 mRNA was isolated with an mRNA Capture kit (Roche) and cDNA was synthesized with
402 a reverse-transcriptase kit (Promega) and PCR amplification was performed in the
403 presence of SYBR green in a 7500 Fast Realtime PCR System (ABI). Specific primers
404 were designed with Primer Express 2.0 (Applied Biosystems). Primer sequences used for
405 mRNA expression were for gene product: GAPDH, forward primer

406 (CCATGTTCGTCATGGGTGTG), reverse primer (GGTGCTAA GCAGTTGGTGGTG).
407 For gene product: ACE2, forward primer (GGACCCAGGAAATGTTCAGA), reverse primer
408 (GGCTGCAGAAAGTGACATGA). For gene product: Syndecan 1, forward primer
409 (ATCACCTTGTCACAGCAGACCC) reverse primer (CTCCACTTCTGGCAGGACTACA).
410 Syndecan 4, forward primer (AGGTGTCAATGTCCAGCACTGTG) reverse primer
411 (AGCAGTAGGATCAGGAAGACGGC). The normalized amount of target mRNA was
412 calculated from the Ct values obtained for both target and household mRNA with the
413 equation Nt = 2Ct(GAPDH) − Ct(target). For relative mRNA expression, control siRNA
414 sample was set at 1 for each donor.
415
416 *RNA interference*
417 Huh7.5 cells were silenced by electroporation with Neon Transfection System (Thermo
418 Fischer Scientific) according to the manufacturers protocol The siRNA (SMARTpool;
419 Dharmacon) were specific for Syndecan 1 (10 µM siRNA, M-010621-01-0005,
420 SMARTpool; Dharmacon), Syndecan 4 (10 µM siRNA, M-003706-01-0005, SMARTpool;
421 Dharmacon) whereas non-targeting siRNA (D-001206-13, SMARTpool; Dharmacon)
422 served as control. Cells were used for experiments 48 hours after silencing and silencing
423 efficiency of the specific targets was verified by real-time PCR and flow cytometry.
424
425 *Biosynthesis inhibition and enzymatic treatment*
426 HuH7.5 cells were treated in D-PBS/0.25% BSA with 46 miliunits heparinase III (Amsbio)
427 for 1 hour at 37°C, washed and used in subsequent experiments. Enzymatic digestion
428 was verified by flow cytometry using antibodies directed against heparan sulfates and
429 digested heparan sulfates.
430
431 *Statistics*
432 A two-tailed, parametric Student's *t*-test for paired observations (differences within the
433 same donor) or unpaired observation (differences between different donors) was
434 performed. For unpaired, non-parametric observations a one-way ANOVA or two-way
435 ANOVA test were performed. Statistical analyses were performed using GraphPad Prism
436 8 software and significance was set at *P< 0.05, **P<0.01***P<0.001****P<0.0001.
437
438

Study approval

This study was performed according to the Amsterdam University Medical Centers, location AMC Medical Ethics Committee guidelines and all donors for blood, skin and BAL gave written informed consent in accordance with the Declaration of Helsinki.

Author Contributions

M.B-J and J.E conceived and designed experiments; M.B-J, J.E, T.M.K, L.C.H, J.L.v.H performed the experiments and contributed to scientific discussion; P.J.M.B., G.J.d.B, R.W.S., M.J.v.G, B.M.N and N.A.K contributed essential research materials and scientific input. M.B-J, J.E, T.M.K and T.B.H.G analyzed and interpreted data; J.E, M.B-J and T.B.H.G. wrote the manuscript with input from all listed authors. T.B.H.G. was involved in all aspects of the study.

Acknowledgements

We thank Jonne Snitselaar and Yoann Aldon for help with production of antibodies and Rene Jonkers and Peter Bonta for conducting the BAL.

Funding

This research was funded by the European Research Council (Advanced grant 670424 to T.B.H.G.), Amsterdam UMC PhD grant and two COVID-19 grants from the Amsterdam institute for Infection & Immunity (to T.B.H.G., R.W.S. and M.J.v.G.). This study was also supported by the Netherlands Organization for Scientific Research (NWO) through a Vici grant (to R.W.S.), and by the Bill & Melinda Gates Foundation through the Collaboration for AIDS Vaccine Discovery (CAVD), grant INV-002022 (to R.W.S.).

Competing interests

There have no conflicts of interest.

Data and materials availability

Reagents and materials presented in this study are available from the corresponding authors under a MTA with the Amsterdam UMC.

471 **References**

472 1. P. Zhou *et al.*, A pneumonia outbreak associated with a new coronavirus of probable bat
473 origin. *Nature* **579**, 270-273 (2020).
474 2. K. Yuki, M. Fujiogi, S. Koutsogiannaki, COVID-19 pathophysiology: A review. *Clin Immunol*
475 **215**, 108427 (2020).
476 3. N. Zhu *et al.*, A Novel Coronavirus from Patients with Pneumonia in China, 2019. *N Engl J*
477 *Med* **382**, 727-733 (2020).
478 4. M. Nicola *et al.*, The socio-economic implications of the coronavirus pandemic (COVID-
479 19): A review. *Int J Surg* **78**, 185-193 (2020).
480 5. World Health Organization (2020) Timeline of WHO's response to COVID-19.
481 6. H. Harapan *et al.*, Coronavirus disease 2019 (COVID-19): A literature review. *J Infect Public*
482 *Health* **13**, 667-673 (2020).
483 7. M. Ferioli *et al.*, Protecting healthcare workers from SARS-CoV-2 infection: practical
484 indications. *Eur Respir Rev* **29** (2020).
485 8. J. S. Peiris, K. Y. Yuen, A. D. Osterhaus, K. Stöhr, The severe acute respiratory syndrome.
486 *N Engl J Med* **349**, 2431-2441 (2003).
487 9. K. P. Y. Hui *et al.*, Tropism, replication competence, and innate immune responses of the
488 coronavirus SARS-CoV-2 in human respiratory tract and conjunctiva: an analysis in ex-vivo
489 and in-vitro cultures. *Lancet Respir Med* 10.1016/s2213-2600(20)30193-4 (2020).
490 10. M. M. Lamers *et al.*, SARS-CoV-2 productively infects human gut enterocytes. *Science*
491 10.1126/science.abc1669 (2020).
492 11. L. Wright, A. Steptoe, D. Fancourt, Are we all in this together? Longitudinal assessment of
493 cumulative adversities by socioeconomic position in the first 3 weeks of lockdown in the
494 UK. *J Epidemiol Community Health* 10.1136/jech-2020-214475 (2020).
495 12. S. K. Brooks *et al.*, The psychological impact of quarantine and how to reduce it: rapid
496 review of the evidence. *Lancet* **395**, 912-920 (2020).
497 13. M. Letko, A. Marzi, V. Munster, Functional assessment of cell entry and receptor usage
498 for SARS-CoV-2 and other lineage B betacoronaviruses. *Nat Microbiol* **5**, 562-569 (2020).
499 14. R. J. Hulswit, C. A. de Haan, B. J. Bosch, Coronavirus Spike Protein and Tropism Changes.
500 *Adv Virus Res* **96**, 29-57 (2016).
501 15. B. J. Bosch, R. van der Zee, C. A. de Haan, P. J. Rottier, The coronavirus spike protein is a
502 class I virus fusion protein: structural and functional characterization of the fusion core
503 complex. *J Virol* **77**, 8801-8811 (2003).
504 16. F. Li, W. Li, M. Farzan, S. C. Harrison, Structure of SARS coronavirus spike receptor-binding
505 domain complexed with receptor. *Science* **309**, 1864-1868 (2005).
506 17. N. Wang *et al.*, Structure of MERS-CoV spike receptor-binding domain complexed with
507 human receptor DPP4. *Cell Res* **23**, 986-993 (2013).
508 18. C. Burkard *et al.*, Coronavirus cell entry occurs through the endo-/lysosomal pathway in a
509 proteolysis-dependent manner. *PLoS Pathog* **10**, e1004502 (2014).
510 19. S. Xia *et al.*, Inhibition of SARS-CoV-2 (previously 2019-nCoV) infection by a highly potent
511 pan-coronavirus fusion inhibitor targeting its spike protein that harbors a high capacity to
512 mediate membrane fusion. *Cell Res* **30**, 343-355 (2020).
513 20. M. Hoffmann *et al.*, SARS-CoV-2 Cell Entry Depends on ACE2 and TMPRSS2 and Is Blocked
514 by a Clinically Proven Protease Inhibitor. *Cell* **181**, 271-280.e278 (2020).

515 21. I. Hamming *et al.*, Tissue distribution of ACE2 protein, the functional receptor for SARS
516 coronavirus. A first step in understanding SARS pathogenesis. *J Pathol* **203**, 631-637
517 (2004).
518 22. X. Zou *et al.*, Single-cell RNA-seq data analysis on the receptor ACE2 expression reveals
519 the potential risk of different human organs vulnerable to 2019-nCoV infection. *Front*
520 *Med* **14**, 185-192 (2020).
521 23. P. J. M. Brouwer *et al.*, Potent neutralizing antibodies from COVID-19 patients define
522 multiple targets of vulnerability. *Science* **369**, 643-650 (2020).
523 24. G. Roderiquez *et al.*, Mediation of human immunodeficiency virus type 1 binding by
524 interaction of cell surface heparan sulfate proteoglycans with the V3 region of envelope
525 gp120-gp41. *J Virol* **69**, 2233-2239 (1995).
526 25. A. Milewska *et al.*, Human coronavirus NL63 utilizes heparan sulfate proteoglycans for
527 attachment to target cells. *J Virol* **88**, 13221-13230 (2014).
528 26. J. Jiang *et al.*, Hepatitis C virus attachment mediated by apolipoprotein E binding to cell
529 surface heparan sulfate. *J Virol* **86**, 7256-7267 (2012).
530 27. A. P. Byrnes, D. E. Griffin, Binding of Sindbis virus to cell surface heparan sulfate. *J Virol*
531 **72**, 7349-7356 (1998).
532 28. B. M. Nijmeijer *et al.*, Syndecan 4 Upregulation on Activated Langerhans Cells Counteracts
533 Langerin Restriction to Facilitate Hepatitis C Virus Transmission. *Front Immunol* **11**, 503
534 (2020).
535 29. A. K. Kakkar, Low- and ultra-low-molecular-weight heparins. *Best Pract Res Clin Haematol*
536 **17**, 77-87 (2004).
537 30. N. Tang *et al.*, Anticoagulant treatment is associated with decreased mortality in severe
538 coronavirus disease 2019 patients with coagulopathy. *J Thromb Haemost* **18**, 1094-1099
539 (2020).
540 31. G. J. Merli, J. B. Groce, Pharmacological and clinical differences between low-molecular-
541 weight heparins: implications for prescribing practice and therapeutic interchange. *P t* **35**,
542 95-105 (2010).
543 32. Q. Wang *et al.*, Structural and Functional Basis of SARS-CoV-2 Entry by Using Human ACE2.
544 *Cell* **181**, 894-904.e899 (2020).
545 33. H. Zhang, J. M. Penninger, Y. Li, N. Zhong, A. S. Slutsky, Angiotensin-converting enzyme 2
546 (ACE2) as a SARS-CoV-2 receptor: molecular mechanisms and potential therapeutic
547 target. *Intensive Care Med* **46**, 586-590 (2020).
548 34. H. P. Jia *et al.*, ACE2 receptor expression and severe acute respiratory syndrome
549 coronavirus infection depend on differentiation of human airway epithelia. *J Virol* **79**,
550 14614-14621 (2005).
551 35. H. Chu *et al.*, Comparative replication and immune activation profiles of SARS-CoV-2 and
552 SARS-CoV in human lungs: an ex vivo study with implications for the pathogenesis of
553 COVID-19. *Clin Infect Dis* 10.1093/cid/ciaa410 (2020).
554 36. K. S. Jones, C. Petrow-Sadowski, Y. K. Huang, D. C. Bertolette, F. W. Ruscetti, Cell-free
555 HTLV-1 infects dendritic cells leading to transmission and transformation of CD4(+) T cells.
556 *Nat Med* **14**, 429-436 (2008).
557 37. C. M. Ribeiro *et al.*, Receptor usage dictates HIV-1 restriction by human TRIM5α in
558 dendritic cell subsets. *Nature* **540**, 448-452 (2016).

559 38. A. Marzi *et al.*, DC-SIGN and DC-SIGNR interact with the glycoprotein of Marburg virus and
560 the S protein of severe acute respiratory syndrome coronavirus. *J Virol* **78**, 12090-12095
561 (2004).
562 39. L. de Witte *et al.*, Langerin is a natural barrier to HIV-1 transmission by Langerhans cells.
563 *Nat Med* **13**, 367-371 (2007).
564 40. R. Sarrami-Forooshani *et al.*, Human immature Langerhans cells restrict CXCR4-using HIV-
565 1 transmission. *Retrovirology* **11**, 52 (2014).
566 41. M. Merad, F. Ginhoux, M. Collin, Origin, homeostasis and function of Langerhans cells and
567 other langerin-expressing dendritic cells. *Nat Rev Immunol* **8**, 935-947 (2008).
568 42. T. B. Geijtenbeek *et al.*, DC-SIGN, a dendritic cell-specific HIV-1-binding protein that
569 enhances trans-infection of T cells. *Cell* **100**, 587-597 (2000).
570 43. S. Bacsa *et al.*, Syndecan-1 and syndecan-2 play key roles in herpes simplex virus type-1
571 infection. *J Gen Virol* **92**, 733-743 (2011).
572 44. K. Hayashida, D. R. Johnston, O. Goldberger, P. W. Park, Syndecan-1 expression in
573 epithelial cells is induced by transforming growth factor beta through a PKA-dependent
574 pathway. *J Biol Chem* **281**, 24365-24374 (2006).
575 45. Y. H. Teng, R. S. Aquino, P. W. Park, Molecular functions of syndecan-1 in disease. *Matrix*
576 *Biol* **31**, 3-16 (2012).
577 46. C. Mycroft-West *et al.*, The 2019 coronavirus (SARS-CoV-2) surface protein (Spike) S1
578 Receptor Binding Domain undergoes conformational change upon heparin binding.
579 http://dx.doi.org/10.1101/2020.02.29.971093.
580 47. L. J. Partridge, L. R. Green, P. N. Monk, Unfractionated heparin potently inhibits the
581 binding of SARS-CoV-2 spike protein to a human cell line.
582 http://dx.doi.org/10.1101/2020.05.21.107870.
583 48. L. Liu *et al.*, SARS-CoV-2 spike protein binds heparan sulfate in a length- and sequence-
584 dependent manner. http://dx.doi.org/10.1101/2020.05.10.087288.
585 49. H. Li *et al.*, SARS-CoV-2 and viral sepsis: observations and hypotheses. *Lancet* **395**, 1517-
586 1520 (2020).
587 50. G. J. Randolph, V. Angeli, M. A. Swartz, Dendritic-cell trafficking to lymph nodes through
588 lymphatic vessels. *Nat Rev Immunol* **5**, 617-628 (2005).
589 51. L. Wu, V. N. KewalRamani, Dendritic-cell interactions with HIV: infection and viral
590 dissemination. *Nat Rev Immunol* **6**, 859-868 (2006).
591 52. C. Chute *et al.*, Syndecan-1 induction in lung microenvironment supports the
592 establishment of breast tumor metastases. *Breast Cancer Res* **20**, 66 (2018).
593 53. Q. Shi, J. Jiang, G. Luo, Syndecan-1 serves as the major receptor for attachment of
594 hepatitis C virus to the surfaces of hepatocytes. *J Virol* **87**, 6866-6875 (2013).
595 54. L. de Witte *et al.*, Syndecan-3 is a dendritic cell-specific attachment receptor for HIV-1.
596 *Proc Natl Acad Sci U S A* **104**, 19464-19469 (2007).
597 55. Z. Zhai *et al.*, Prevention and Treatment of Venous Thromboembolism Associated with
598 Coronavirus Disease 2019 Infection: A Consensus Statement before Guidelines. *Thromb*
599 *Haemost* **120**, 937-948 (2020).
600 56. World Health Organization (2020) Clinical management of COVID-19. Interim guidance 27
601 May 2020. (World Health Organization), p 62.
602 57. Z. Zhang, C. Coomans, G. David, Membrane heparan sulfate proteoglycan-supported
603 FGF2-FGFR1 signaling: evidence in support of the "cooperative end structures" model. *J*
604 *Biol Chem* **276**, 41921-41929 (2001).

605 58. B. D. Lindenbach *et al.*, Complete replication of hepatitis C virus in cell culture. *Science*
606 **309**, 623-626 (2005).
607 59. Y. Aldon *et al.*, Rational Design of DNA-Expressed Stabilized Native-Like HIV-1 Envelope
608 Trimers. *Cell Rep* **24**, 3324-3338.e3325 (2018).
609 60. A. W. Mesman *et al.*, Measles virus suppresses RIG-I-like receptor activation in dendritic
610 cells via DC-SIGN-mediated inhibition of PP1 phosphatases. *Cell Host Microbe* **16**, 31-42
611 (2014).

612

613

614

615 **Figures 1 to 6**

616 **Figure 1**

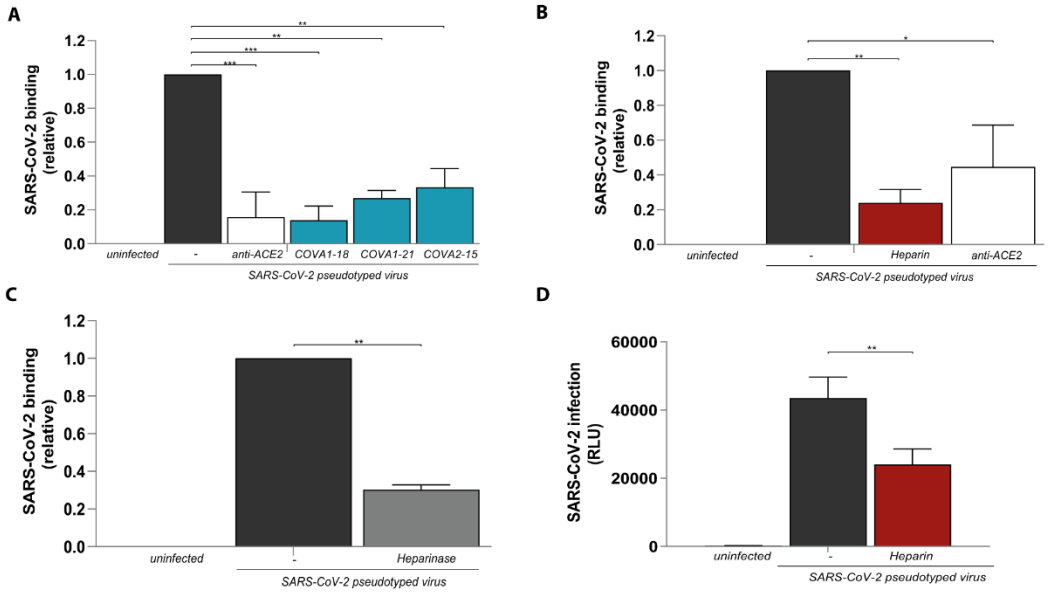

Figure 1. Heparan sulfates are crucial for SARS-CoV-2 binding and infection.
(**A-B**) Huh 7.5 cells were preincubated with neutralizing antibody to ACE2 and SARS-CoV-2 pseudovirus was pre-incubated with mAb COVA1-18, COVA1-21 and COVA2-15 or UF heparin (250IU). Cells were infected with SARS-CoV-2 pseudovirus and binding was determined by ELISA. (**C**) Heparan sulfates were removed from Huh 7.5 cells by heparinase treatment and SARS-CoV-2 pseudovirus binding was determined. Error bars are the mean ± SEM from three independent experiments. (**D**) Huh 7.5 cells were infected with SARS-CoV-2 pseudovirus and infection was measured after 5 days of culture by luciferase assay. Virus was pretreated with heparin (250IU). Data show the mean values and error bars are the SEM. Statistical analysis was performed using (**A**) ordinary one-way ANOVA with Tukey multiple-comparison test. ***p= 0.0006, ***p= 0.0005, **p= 0.0018, **p= 0.0036 (n = 3), (**B**) **p= 0.0010, *p= 0.0255 (n=4), (**C**) two-tailed, unpaired Student's t-test with Welch's correction. **p= 0.0012 (n = 3), (**D**) ordinary one-way ANOVA with Tukey multiple-comparison test. **p= 0.0085 (n=6 measured in triplicate). RLU: relative light units.

617

618

619 **Figure 2**

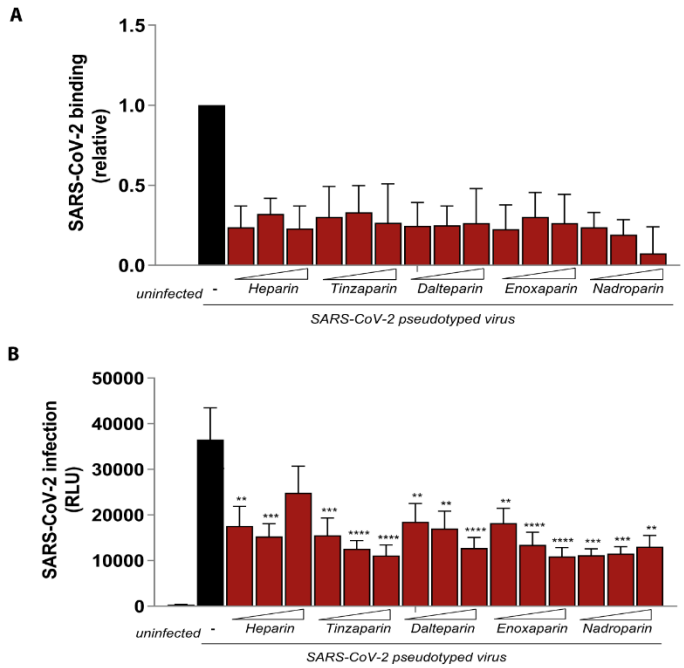

Figure 2. LMWH block binding and infection by SARS-CoV-2.
SARS-CoV-2 was pretreated with UF heparin and different LMWH at different concentrations (50-100-250IU) and (**A**) binding to Huh 7.5 cells was determined or (**B**) infection was measured after 5 days by ELISA or luciferase assay, respectively. Data show the mean values and error bars are the SEM. Statistical analysis was performed using (**A**) ordinary one-way ANOVA with Tukey's multiple-comparison test. (n = 3), (**B**) ordinary one-way ANOVA with Dunnett's multiple-comparison test. **p= 0.0018, ***p= 0.0003, ***p= 0.0004, ****p< 0.0001, **p= 0.0036, **p= 0.0012, **p= 0.0029 (n = 3 donors measured in triplicate). RLU: relative light units.

620

621

622

623 **Figure 3**

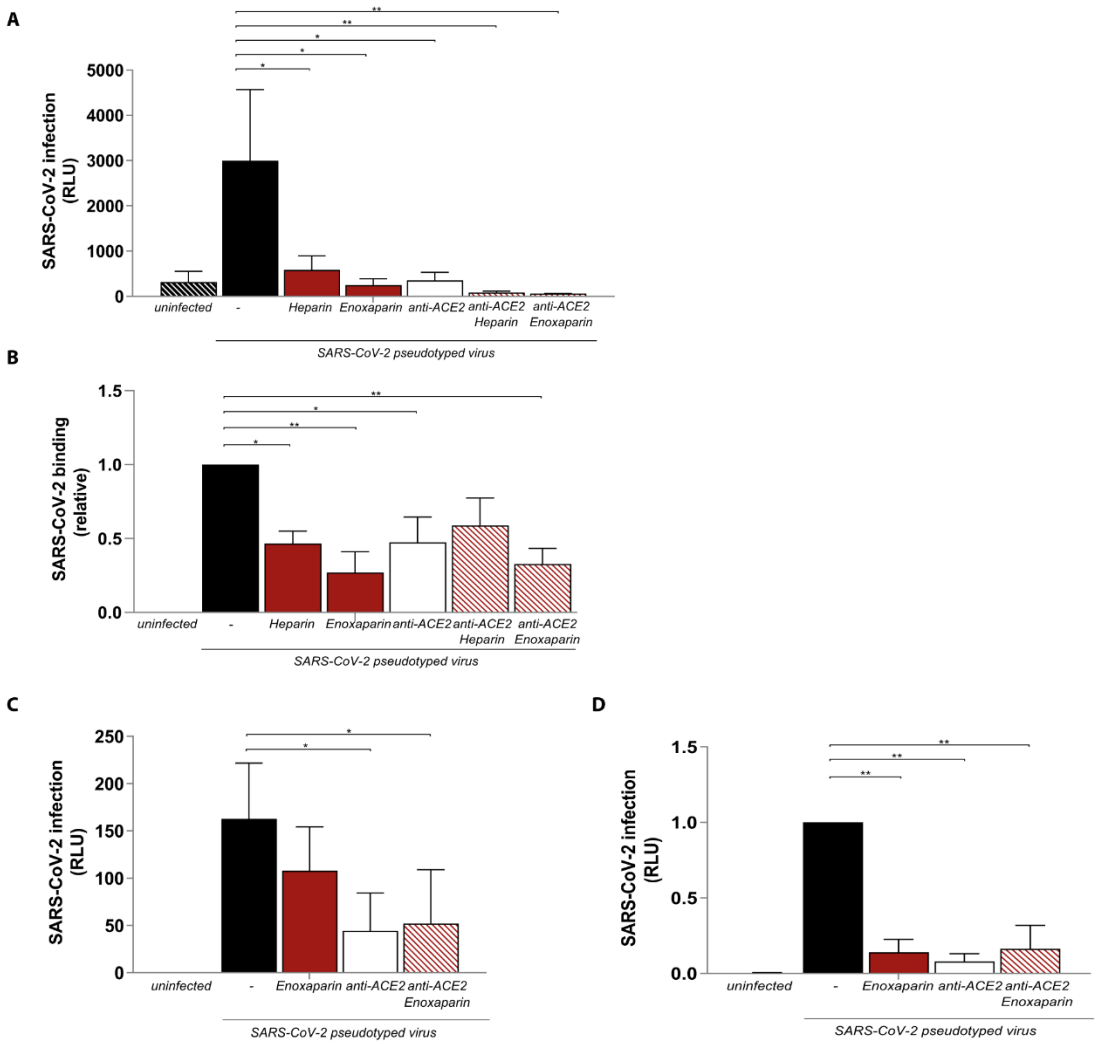

Figure 3. SARS-CoV-2 binding and infection of epithelial cells is blocked by UF heparin and LMWH
(**A**) 293T cells expressing ACE2 were infected with SARS-CoV-2 in presence or absence of antibodies against ACE2, UF heparin (250IU) or enoxaparin (250IU). (**B**) SARS-CoV-2 binding to was determined in presence of antibodies against ACE2, UF heparin (250IU) or enoxaparin (250IU). (**C-D**) SARS-CoV-2 infection was measured in undifferentiated or polarized Caco2 cells in presence of antibodies against ACE2, and UF heparin (250IU) or enoxaparin (250IU). Data show the mean values and error bars are the SEM. Statistical analysis was performed using (**A**) ordinary one-way ANOVA with Dunnett's multiple-comparison test. *p= 0.0380, *p= 0.0136, *p= 0.0189, **p= 0.0080, **p= 0.0074 (n = 3 measured in triplicates), (**B**) ordinary one-way ANOVA with Dunnett's multiple-comparison test. *p= 0.0466, **p= 0.0069, *p= 0.0181, **p= 0.0046, (n = 3 donors), (**C**) unpaired Mann Whitney test. *p= 0.0331, *p= 0.0258 (n = 3 measured in triplicates), (**D**) ordinary one-way ANOVA with Tukey's multiple-comparison test. **p= 0.0013, **p= 0.0018, **p= 0.0021 (n = 3 donors measured in triplicate). RLU: relative light units.

624

625

626 **Figure 4**

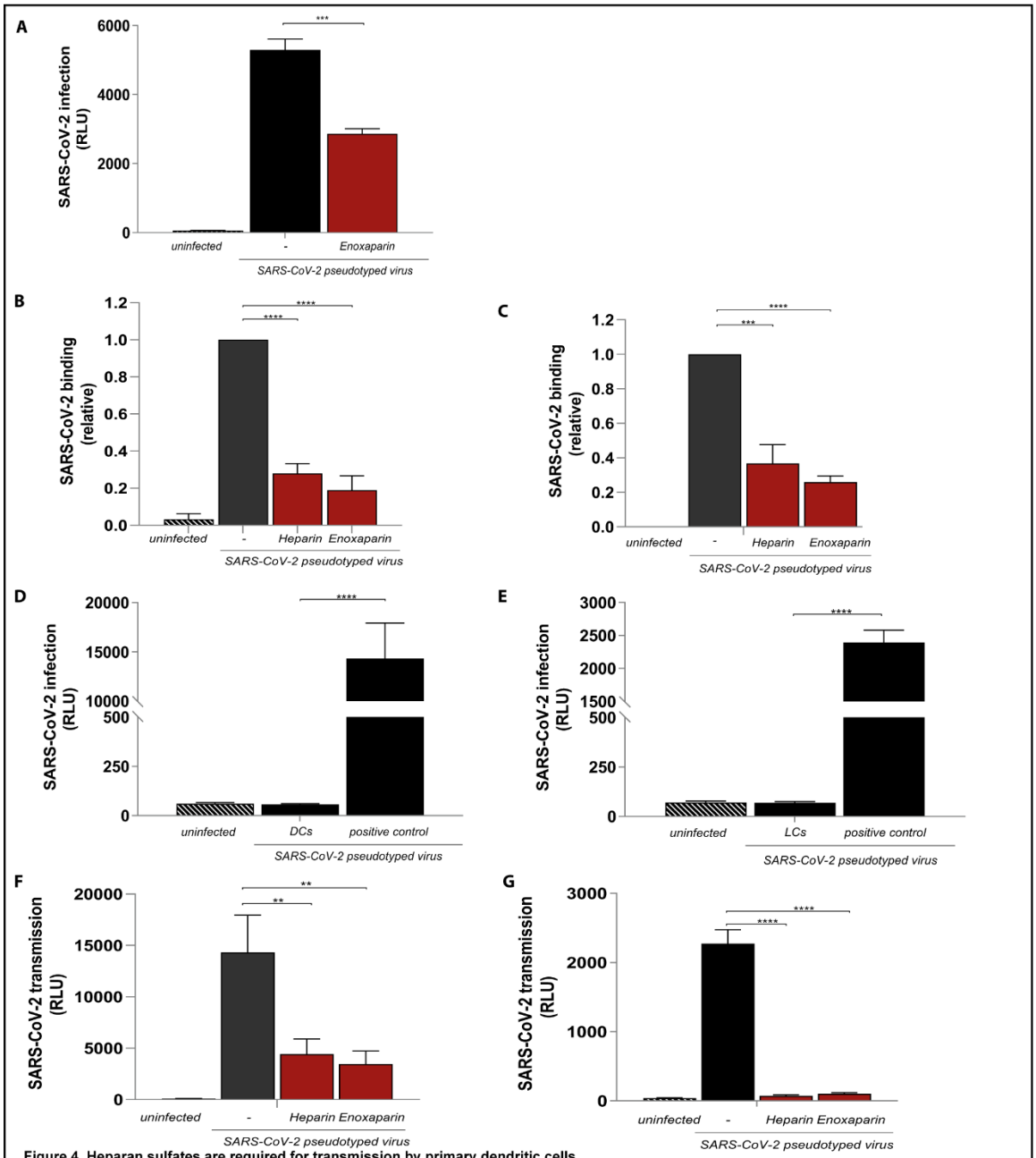

Figure 4. Heparan sulfates are required for transmission by primary dendritic cells.
(**A**) Alveolar macrophages (BAL) infected with SARS-CoV-2 and infection was measured after 5 days. One representative donor out of 3 is depicted. (**B-C**) SARS-CoV-2 binding to monocyte-derived DCs (**B**) and primary LCs (**C**) in presence of UF heparin (250IU) or enoxaparin (250IU). (**D-E**) DCs (**D**) and LCs (**E**) were infected with SARS-CoV-2 and infection was measured after 5 days. As positive controls Huh 7.5 cells were infected. (**F-G**) DCs (**F**) and LCs (**G**) were preincubated with SARS-CoV-2 pseudovirus for 4 h in presence or absence of UF heparin (250 IU) or enoxaparin (250 IU), extensively washed and co-cultured with Huh 7.5 cells. Transmission by DCs or LCs to Huh 7.5 cells was determined by luciferase assay. Data show the mean values and error bars are the SEM. Statistical analysis was performed using (**A**) ordinary one-way ANOVA with Tukey's multiple-comparison test. ***p= 0.0004 (n = 1), (**B-C**) ordinary one-way ANOVA with Tukey's multiple-comparison test. (**B**)****p< 0.0001, (**C**) ***p= 0.0002, ****p< 0.0001 (n = 4), (**D-E**) ordinary one-way ANOVA with Tukey's multiple-comparison test. ****p< 0.0001 (**D**) n=4 measured in triplicate and (**E**) n = 3 donors measured in duplicate, (**F**) ordinary one-way ANOVA with Dunnett's multiple-comparison test. **p= 0.0042, **p= 0.0016 (n = 4 measured in triplicate), (**G**) ordinary one-way ANOVA with Tukey's multiple-comparison test.)****p< 0.0001 (n = 3 measured in triplicate). DCs: Dendritic cells, LCs: Langerhans cells, RLU: relative light units.

627

628

629 **Figure 5**

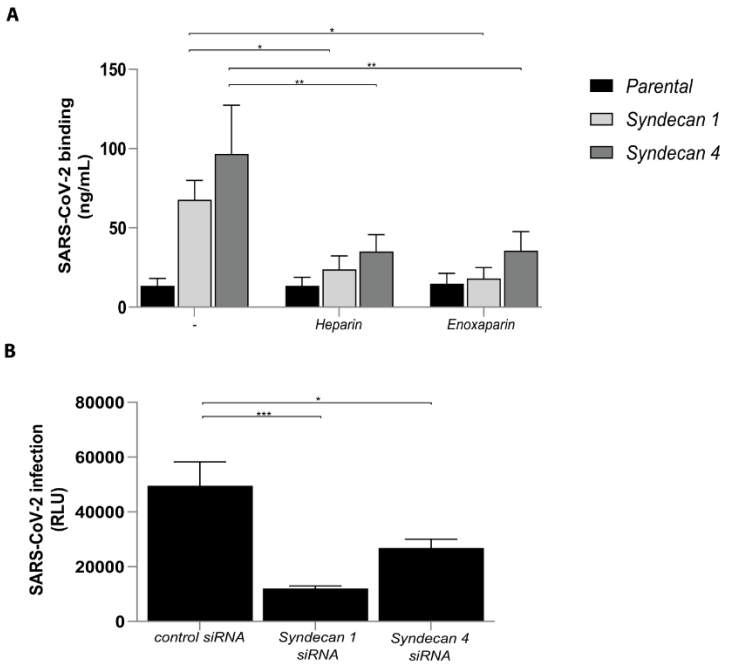

Figure 5. Heparan sulfate proteoglycans Syndecan 1 and 4 are important for SARS-CoV-2 binding and infection
(**A**) Namalwa cells ectopically expressing either Syndecan 1 or 4 were exposed to SARS-CoV-2 pseudovirus, in presence or absence of UF heparin (250IU) or enoxaparin (250IU and binding was measured after 4h. (**B**) Syndecan 1 and 4 were silenced by RNA interference in Huh7.5 cells and infection with SARS-CoV-2 pseudovirus was measured after 5 days. Representative data for an experiment repeated more than three times with similar results. Data show the mean values and error bars are the SEM. Statistical analysis was performed using (**A**) 2way-ANOVA with Dunnett's multiple-comparison test. *p= 0.0408, *p= 0.0189, **p= 0.0032, **p= 0.0035 (n = 7), (**B**) 2way-ANOVA with Tukey's multiple-comparison test. ***p= 0.0002, *p= 0.0124. (n = 1 measured in triplicate). siRNA: RNA interference, RLU: relative light units.

630

631

632 **Figure 6**

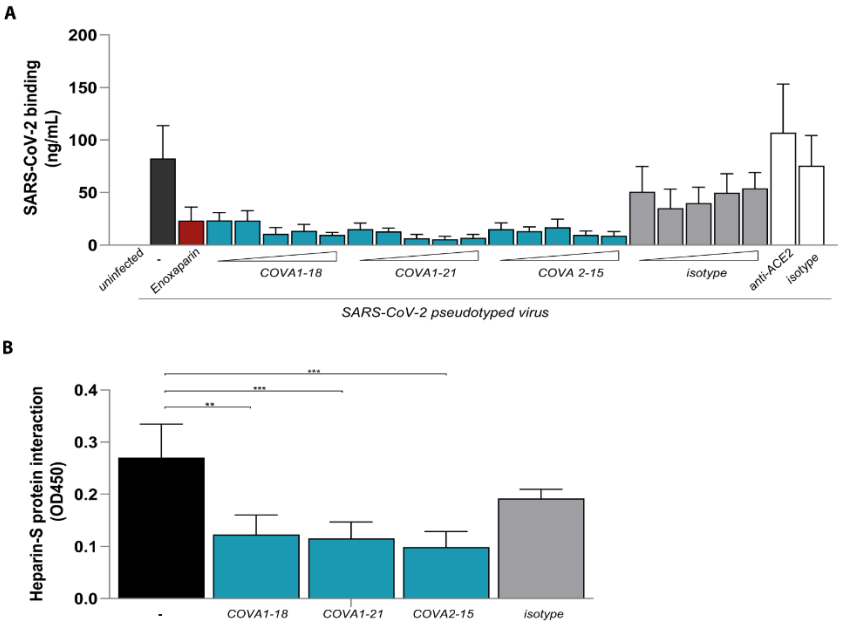

Figure 6. Neutralizing antibodies against SARS-CoV-2 block heparan sulfate binding.
(**A**) SARS-CoV-2 pseudovirus was treated with neutralizing antibodies against SARS-CoV-2 (COVA1-18, COVA1-21 and COVA2-15) and isotype control (VRC01 in grey) at concentrations 0.05, 0.1, 0.5, 1 and 5 µg/mL, while Syndecan 1 expressing Namalwa cells were preincubated with anti-ACE2 antibody and it corresponding isotype (both in white). Binding was determined by ELISA. (**B**) The ability of the neutralizing antibodies to prevent SARS-CoV-2 S protein binding to heparan sulfates was measured in the Heparin-SARS-CoV-2 S protein binding assay. S protein was preincubated with the different neutralizing antibodies (COVA1-18, COVA1-21 and COVA2-15) and isotype control (VRC01) and binding was determined. Data show the mean values and error bars are the SEM. Statistical analysis was performed using (**A**) ordinary one-way ANOVA with Tukey's multiple-comparison test. (n = 3), (**B**) 2way-ANOVA with Tukey's multiple-comparison test. **p= 0.0019, ***p= 0.0010, ***p= 0.0002. (n = 2 measured in duplicates).

633

634

635

636 **Supplementary Figures 1 to 2**

637 **Supplementary Figure 1**

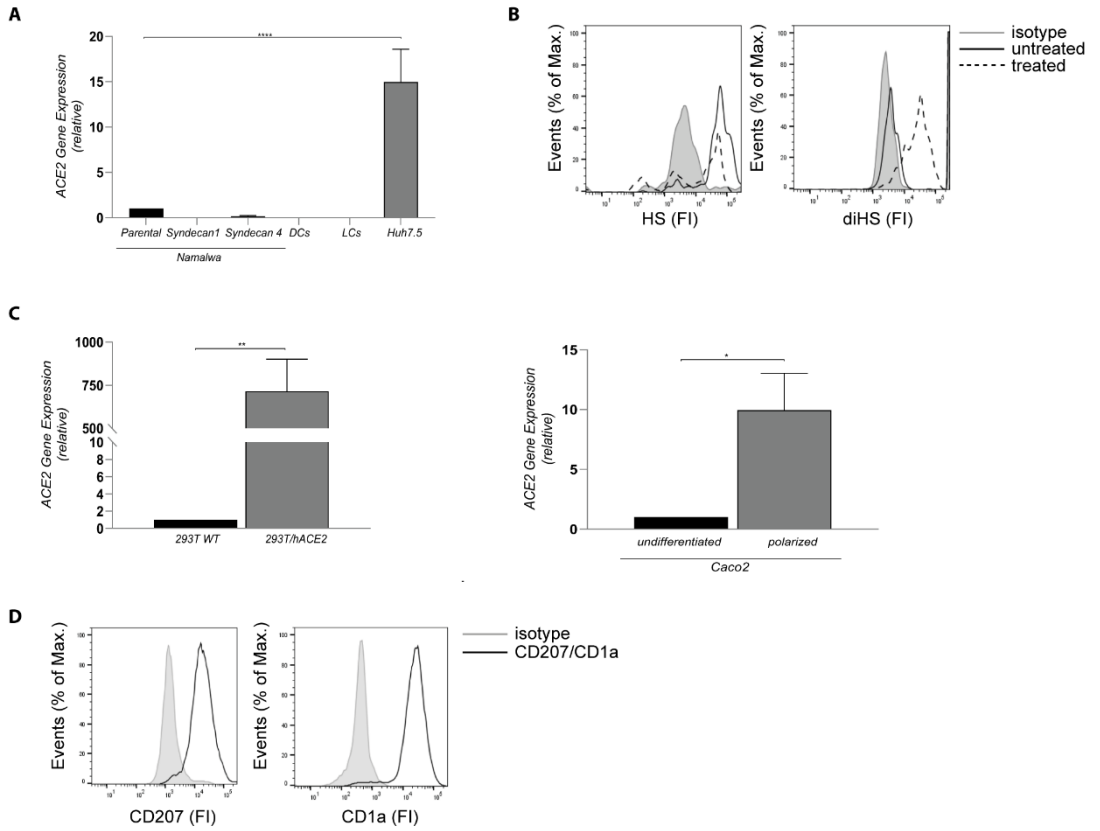

Supplementary Fig.1
(**A**) ACE2 cell surface expression on Namalwa cell line, DCs, LCs and Huh 7.5. Representative data for an experiment repeated more than three times with similar results. (**B**) Huh7.5 were left untreated or treated with heparinase for 1 h and heparan sulfate or digested heparan sulfate expression was determined by flow cytometry. One representative donor out of 3 is depicted. (**C**) Cell surface expression of ACE2 on 293T and Caco2 cell lines was determined by real-time PCR. (**D**) LC were stained with antibodies against CD207 and CD1a and analysed by flow cytometry. The histogram shows the cell surface expression of the receptor. Representative data for an experiment repeated more than three times with similar results. Data show the mean values and error bars are the SEM. Statistical analysis was performed using (**A**) ordinary one-way ANOVA with Tukey's multiple-comparison test. ****$p < 0.0001$ (n = 1), (**C**) two-tailed, unpaired Student's t-test. **$p=0.0086$ (n = 3), *$p=0.0198$ (n=3). DCs: Dendritic cells, LCs: Langerhans cells

638

639 **Supplementary Figure 2**

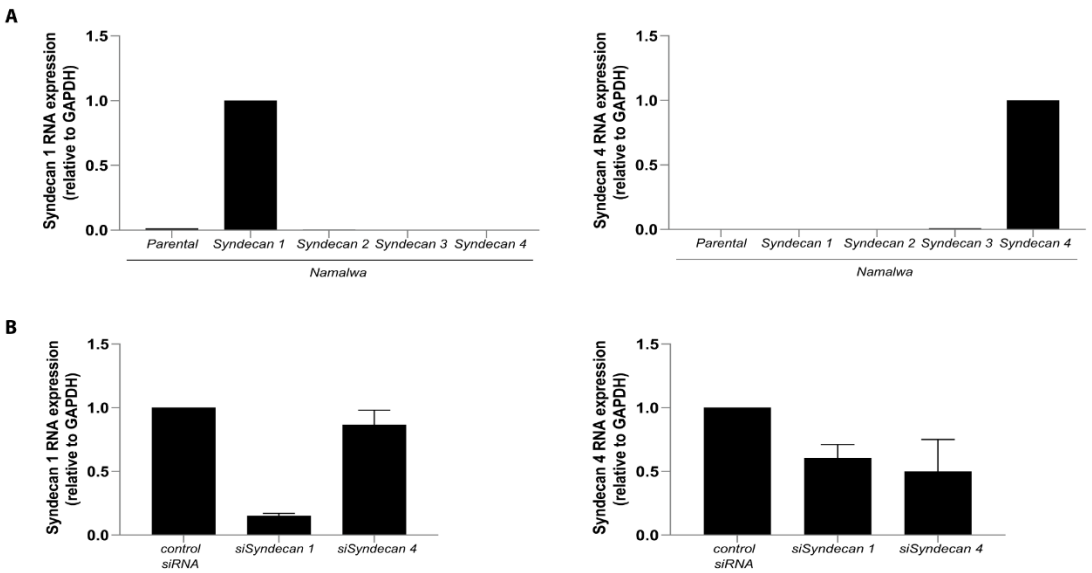

Supplementary Fig.2
(**A**) Different Namalwa Syndecan cell lines express Syndecan 1 - 4, on the cell surface determined by real-time PCR. (**B**) Syndecan 1 and 4 silencing was confirmed by real-time PCR. mRNA expression was normalized to GAPDH and set at 1 in cells treated with control siRNA. Representative data for an experiment repeated more than three times with similar results.

640